applied sciences

MDPI

Article

Weightage Effect during Back-Calculation of Rock-Mass Quality from the Installed Tunnel Support in Rock-Mass Rating and Tunneling Quality Index System

Jonguk Kim [1], Hafeezur Rehman [1,2], Wahid Ali [2], Abdul Muntaqim Naji [1,3] and Hankyu Yoo [1,*]

[1] Department of Civil and Environmental Engineering, Hanyang University, ERICA Campus, Sangnok–gu, Ansan 15588, Korea; jonggia@naver.com (J.K.); miner1239@yahoo.com (H.R.); engineernaji@gmail.com (A.M.N.)

[2] Department of Mining Engineering, Baluchistan University of Information Technology Engineering and Management Sciences (BUITEMS), Quetta 081, Pakistan; wahid-mrh@hotmail.com

[3] Department of Geological Engineering, Baluchistan University of Information Technology Engineering and Management Sciences (BUITEMS), Quetta 081, Pakistan

* Correspondence: hankyu@hanyang.ac.kr; Tel.: +82-31-400-5147; Fax: +82-31-409-4104

Received: 17 April 2019; Accepted: 16 May 2019; Published: 19 May 2019

Abstract: In extensively used empirical rock-mass classification systems, the rock-mass rating (*RMR*) and tunneling quality index (*Q*) system, rock-mass quality, and tunnel span are used for the selection of rock bolt length and spacing and shotcrete thickness. In both systems, the rock bolt spacing and shotcrete thickness selection are based on the same principle, which is used for the back-calculation of the rock-mass quality. For back-calculation, there is no criterion for the selection of rock-bolt-spacing-based rock-mass quality weightage and shotcrete thickness along with tunnel-span-based rock-mass quality weightage. To determine this weightage effect during the back-calculation, five weightage cases are selected, explained through example, and applied using published data. In the *RMR* system, the weightage effect is expressed in terms of the difference between the calculated and back-calculated rock-mass quality in the two versions of *RMR*. In the *Q* system, the weightage effect is presented in plots of stress reduction factor versus relative block size. The results show that the weightage effect during back-calculation not only depends on the difference in rock-bolt-spacing-based rock-mass quality and shotcrete along with tunnel-span-based rock-mass quality, but also on their corresponding values.

Keywords: *RMR*; *Q*; tunnel support; back-calculation; weightage

1. Introduction

The depth of underground excavations is increasing day by day for different civil and mining engineering projects posing more challenges for safe and economic construction [1–3]. The difficulties for modelling such underground excavations due to the complex nature of rock mass are decreasing due to advancement in the research and technology, materials and systems not only in the conventional excavations methods, but also in mechanized one [4–7]. In underground excavations, the issues related to the rock-mass behavior comprise the strength properties of intact rock, joint related aspects, environmental features (ground water and in situ stresses), configuration of the excavation cross section, and the excavation method; furthermore, these issues define the support required for the underground excavation [8,9]. The ability to forecast the rock-mass quality and support pattern during the design of underground excavation is a challenging and risky task [10]. To stabilize these

excavations, researchers characterize the ground in such a manner that is suitable for the support design based on past experiences, which has resulted in the development of different empirical rock-mass classification systems. Till date, empirical rock-mass classification systems have been proposed for the tunnel support system design since the earliest empirical classification proposed by Terzaghi in 1946 known as the rock load classification [4]. Some of the recommended classification systems are not favored by engineers owing to their non-practical application, but few have been frequently used owing to their reliability and practicality. The most extensively used empirical classifications of rock mass during tunnel design and construction in the world are the rock-mass rating (*RMR*) classifications and tunneling quality index (*Q*) systems [11,12]. These two systems for the classification of rock masses used by engineers provide convenience in defining the preliminary support systems. The applicability of these systems has been extended with improvements in tunnel construction technology and these systems are revised extensively either in the form of characterization or support [4].

Based on ground behaviors and the available tools for underground excavation in rock engineering, the application of empirical classification systems are limited to different ground behavior during tunnel excavation and stabilization [8]. In empirical classification systems, fiber-reinforced shotcrete and rock bolts are preliminary supports that are recommended during tunnel design and construction, and *RMR* and *Q* systems are effective tools for this purpose. The updated versions of these two systems suggest the shotcrete thickness and rock bolt spacing based on the same principles [13], as the excavation support ratio (ESR) in the *Q* system is not a parameter that is generally used worldwide, and individual countries have their own respective standards [14]. According to these principles, the fiber-reinforced shotcrete thickness is a function of the rock-mass quality (*RMR* and *Q*) and tunnel span; however, the rock bolt spacing is only a function of the rock-mass quality. During tunnel stability, fiber-reinforced shotcrete and installed rock bolts act as a compound support system and the contribution of individual support depends upon its installation time and distance from the excavation face [15]. Based on the relationships of the rock-mass quality with the spacing of rock bolts (20 mm dimeter) and thickness of fiber-reinforced shotcrete in the support charts of each system, a back analysis approach was established for the determination of the rock-mass quality from the tunnel span, shotcrete thickness, and rock bolt spacing in already supported tunnels [16]. These two relations were used for the back-calculation of the rock-mass quality, and their averaged value (rock-mass quality obtained from shotcrete thickness and tunnel span, and the rock-mass quality obtained from rock bolts spacing) was used for the final calculation of the *RMR** (*RMR* calculated through back-calculation) and *Q** (*Q* value calculated through back-calculation). This averaged value approach is adopted owing to the unavailability of assessment criterion for calculating the rock-mass quality value according to the importance of the support (rock bolt and shotcrete) with the span in the two classification systems.

To extend the application of empirical classification systems (especially *RMR* and *Q*) to different ground behaviors for the tunnel excavation and stability, weightage effect during back-calculation of rock-mass quality is critical. Owing to the unavailability criterion for the final calculations of the rock-mass quality (*RMR** and *Q**), five different cases are taken into consideration in this study to evaluate the weightage effect during the back-calculation of the *RMR** and *Q**. The weightage adopted in Cases 1 and 3 are already considered for the back-calculation of the rock-mass quality in the *Q* system for their extension to a highly stressed jointed rock mass [16,17]. However, in the case of RMR_{89} [18] and RMR_{14} [19], which are the two versions of the *RMR* systems, only the Case 3 weightage was assumed in the rock-mass quality back-calculation for the purpose of their extension. The different assessment cases adopted in this study are plotted, and the effect of the weightage in each case is discussed.

2. Materials and Methods

2.1. RMR Classification System and Tunnel Support Design

As established empirically for the tunnel support design by Z. T. Richard Bieniawski in 1973, the *RMR* classification, also known the geomechanics classification, has been restructured since its

establishment, either in its characterization or recommended support pattern or both [11,16,18–24]. The revised characterization criteria in different version of *RMR* is shown in Table 1 [4]. The RMR_{89}, which is the 1989 form of the *RMR*, is still used as a design tool in rock mechanics, particularly for the classification of a rock mass during tunnel support design; furthermore, its latest version is 2014, which is known as RMR_{14}. As a function of six parameters (R_1–R_6), the RMR_{89} is defined in Equation (1). These six parameters represent the rating for the intact rock uniaxial compressive strength (σ_c), rock quality designation (*RQD*), spacing of joints (χ), condition of these joints, groundwater condition, and relation of tunnel orientation with respect to joint orientation, respectively.

$$RMR_{89} = R_1 + R_2 + R_3 + R_4 + R_5 + R_6 \quad (1)$$

R_1–R_3 in Equation (1) can be calculated from Equations (2)–(4), respectively [13];

$$R_1 = 0.126\sigma_c - 0.0004\sigma_c^2, \ (\sigma_c \leq 110 \text{ MPa}), \quad (2a)$$

$$R_1 = 0.475\sigma_c^{0.626}, \ (\sigma_c \geq 110 \text{ MPa}), \quad (2b)$$

$$R_2 = 0.22RQD - 0.0002RQD^2, \quad (3)$$

$$R_3 = 2.281 \times \ln(x) - 3.41, \ (x = 5\text{–}200 \text{ mm}); \quad (4a)$$

$$R_3 = 4.175 \times \ln(x) - 13.51, \ (x = 200\text{–}900 \text{ mm}); \quad (4b)$$

$$R_3 = 6.250 \times \ln(x) - 27.55, \ (x = 900\text{–}2000 \text{ mm}). \quad (4c)$$

In 2014, a revised structure was proposed for the *RMR* value calculation with some new parameters, as shown in Equation (5), where RMR_b is the basic *RMR*; F_0 is a parameter similar to R_6 in Equation (1); and F_s and F_e are parameters that show the effect of the tunnel excavation method and stress–strain behavior at the tunnel face during their construction [19].

$$RMR_{14} = (RMR_b + F_0) \times F_s \times F_e \quad (5)$$

RMR_b, F_e, and F_s in Equation (5) can be calculated using Equations (6)–(8), respectively:

$$RMR_b = R_1 + R_{2\text{–}3} + R_4 + R_5 + R_I \quad (6)$$

$$F_e = 1 + 2.\left(\frac{RMR}{100}\right)^2, RMR < 40; \quad (7a)$$

$$F_e = 1.32 - \frac{\sqrt{(RMR - 40)}}{25}, \ RMR > 40 \quad (7b)$$

$$F_s = 1.3, \ ICE < 15; \quad (8a)$$

$$F_s = \frac{2.3 \times \sqrt{100 - ICE}}{7.1 + \sqrt{100 - ICE}}, \ 15 < \text{ICE} < 70, \quad (8b)$$

$$F_s = 1, \ ICE > 70 \quad (8c)$$

The parameters $R_{2\text{–}3}$ and R_I in Equation (6) are the ratings for the joint frequency and intact rock alterability. The joint frequency (λ) rating can be calculated using Equation (9). In Equation (8), *ICE* is the abbreviation of a Spanish word Índice de Comportamiento Elástico, which means index of elastic behavior, and this *ICE* is the function of the intact rock strength, in situ stresses, rock-mass quality, and tunnel shape and can be calculated using Equation (10) [25].

$$R_{2\text{–}3} = 34.442 \times e^{-0.046 \times \lambda}, \ (\lambda \leq 20); \quad (9a)$$

$$R_{2\text{–}3} = 22.8 - 0.457 \times \lambda, \ (\lambda \geq 20). \quad (9b)$$

$$ICE = \frac{3704 \times \sigma_c \times e^{\frac{RMR-100}{24}}}{(3 - K_0) \times H} \times F, \ (K_0 \leq 1); \tag{10a}$$

$$ICE = \frac{3704 \times \sigma_{ci} \times e^{\frac{RMR-100}{24}}}{(3 \times K_0 - 1) \times H} \times F, \ K_0 \geq 1. \tag{10b}$$

where H = tunnel depth (m), K_0 = virgin stress ratio, and F = shape coefficient.

In terms of the support design, the major updates in the RMR_{89} application for tunnel support design include expressing the fiber-reinforced shotcrete thickness, rock bolt spacing, and length in the form of charts and equations [24] instead of tables [18]. Equation (11) is used for determining the rock bolt spacing, which shows that their spacing depends on RMR_{89} (rock-mass quality) only. The shotcrete design chart, developed for tunnel support design in the *RMR* system, shows that the shotcrete thickness is influenced by the tunnel span, and RMR_{89} and the weightage of tunnel span and RMR_{89} is influenced by the tunnel span.

$$S_b(m) = 0.5 + 2.5 \times \frac{RMR_{89} - 20}{65}, \ 20 < RMR_{89} \leq 85 \tag{11a}$$

$$S_b(m) = 0.25 + \frac{(RMR_{89} - 10)^{1.5}}{140}, \ 10 < RMR_{89} \leq 20 \tag{11b}$$

$$S_b(m) = 0.25, \ RMR_{89} \leq 10. \tag{11c}$$

Table 1. Characterization criteria in different versions of the rock-mass rating (*RMR*) system.

Parameter		*RMR*							
		1973 [11]	**1974 [20]**	**1975 [21]**	**1979 [22]**	**1989 [18]**	**2011 [23]**	**2013 [24]**	**2014 [19]**
Intact rock strength (MPa)		10–0	10–0	15–0	15–0	15–0	15–0	15–0	15–0
RQD (%)		16–3	20–3	20–3	20–3	20–3	20–0	-	-
Joint spacing (mm)		30–5	30–5	30–5	20–5	20–5	20–0	-	-
Discontinuity density (joints per meter)		-	-	-	-	-	-	40–0	40–0
Separation of joints (mm)		5–1	-	-	-	-	-	-	-
Continuity of joints (m)		5–0	-	-	-	-	-	-	-
Weathering		9–1	-	-	-	-	-	-	-
Condition of joints		-	15–0	25–0	30–0	30–0	30–0	30–0	20–0
Groundwater		10–2	10–2	10–0	15–0	15–0	15–0	15–0	15–0
Alterability (%)		-	-	-	-	-	-	-	10–0
Adjustment	F_0	15–3	15–3	0– (–12)	0– (–12)	0– (–12)	0– (–12)	0– (–12)	0– (–12)
	F_e	-	-	-	-	-	-	-	1.32–1
	F_s	-	-	-	-	-	-	-	1.3–1

2.2. Q System Classification and Tunnel Support Design

The tunneling quality index, also known as the Q system for the classification of rock mass, is the tunneling-data-based empirical classification system used for the tunnel support design [12]. The system groups the ground for the design purpose into nine rock-mass classes. The Q value is calculated using Equation (12) and ranges from a minimum value of 0.001 to a maximum value of 1000:

$$Q = \left(\frac{RQD}{J_n}\right) \times \left(\frac{J_r}{J_a}\right) \times \left(\frac{J_w}{SRF}\right) \tag{12}$$

The main modifications in the structure of Equation (12) since 1974 were made by including a normalized factor owing to the important part of σ_c in the properties of rock mass, and the modified system was represented using Q_c (Equation (13)) [26]:

$$Q_c = \left(\frac{RQD}{J_n}\right) \times \left(\frac{J_r}{J_a}\right) \times \left(\frac{J_w}{SRF}\right) \times \left(\frac{\sigma_c}{100}\right) \quad (13)$$

Since 1974, the tunnel support technology has improved considerably, and with these modifications, the support diagram for the support design of a tunnel has also been revised. In the present position, the support diagram of the Q system shows that the spacing of the rock bolt depends on the Q or Q_c value only; however, the thickness of the shotcrete depends on the D_e value in addition to the Q or Q_c values [27]. In the support chart of the Q system, D_e is the tunnel span divided by the ESR.

2.3. Tunnel Support and Back-Calculation of Rock-Mass Quality

The tunnel span along with the already fixed support (in terms of rock bolt spacing and shotcrete thickness) can be used for the calculation of the rock-mass quality by using the support charts of the two classification systems (*RMR* and *Q*) and Equation (11) [13]. Equation (11) and the support chart of the *Q* system show that the spacing of the rock bolts is based on the rock-mass quality only, and this spacing of rock bolts can be directly used for obtaining the rock-mass quality during (*RMR* and *Q* value) the back-calculation. These back-calculated *RMR* and *Q* values are defined as RMR_1* and Q_1*, respectively, as shown in Figure 1. The spraying of the fiber-reinforced shotcrete is compulsory during tunnel construction, and the thickness of this sprayed fiber-reinforced shotcrete depends on the quality of the rock mass (*Q* or *RMR*) in addition to the tunnel span or D_e. The thickness of this shotcrete along with the tunnel size can also be used to identify the rock-mass quality through the back analysis of an already supported tunnel section based on the support charts of RMR_{89} and *Q* system. These back-calculated *RMR* and *Q* values are as defined RMR_2* and Q_2*, respectively, in Figure 1. During the back-calculation of RMR_1* and Q_1*, only the rock bolt spacing is required. In the case of the back-calculation of RMR_2* and Q_2*, the shotcrete thickness in addition to the supported tunnel span are required. During the RMR_2* and Q_2* calculation, the contribution of the rock-mass quality to the shotcrete thickness is important for the final calculation of the rock-mass quality (*RMR** and *Q**). These values depend on the inclination of a tangent in the shotcrete support line as found in the support charts of *RMR* and *Q* systems, respectively. The final rock-mass quality for both the systems can be evaluated using two different rock-mass quality values (rock-mass quality obtained using rock bolt spacing (RMR_1* and Q_1*) and that obtained using shotcrete thickness (RMR_2* and Q_2*)) through their weightage.

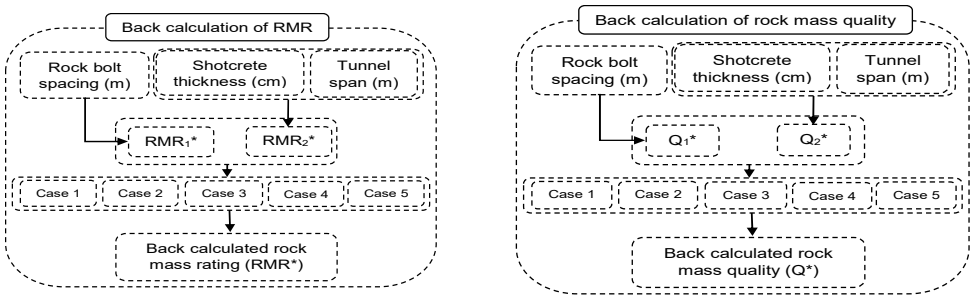

Figure 1. Back-calculation of rock-mass quality (*RMR** and *Q**) based on five different cases, while considering the weightage of the rock-mass quality obtained from the rock bolts spacing and shotcrete thickness along with the tunnel span.

In this study, the data of the four projects named Lowari tunnel (LT), Neelum Jhelum Hydropower (NJHP), Kohat tunnel (KT), and Golengol Hydropower (GGHP) are used. These detailed data that were used for the extension of the *RMR* and *Q* system in a highly stress-jointed rock-mass environment are

available [16]. For the purposes of the extension of the *RMR* system, the *RMR* values were calculated using two different approaches: (1) as per normal procedure of characterization (RMR_{89} and RMR_{14}), and (2) using the back-calculation approach (*RMR**). Following Approach 1, the summary of the RMR_{89} and RMR_{14} values obtained for 542 sections of the four tunneling projects are expressed in Table 2.

Table 2. Summary of rock-mass rating values of RMR_{89} and RMR_{14} for the 542 tunnel sections obtained through rock-mass characterization approach.

Classification System		Project			
		LT	**NJHP**	**KT**	**GGHP**
RMR_{89}	Minimum	45.6	30.5	40.8	48.6
	Maximum	72.64	66.62	72.22	63.19
	Mean	64.0	51.51	62.85	59.48
	Standard Deviation	6.21	7.97	7.53	3.97
RMR_{14}	Minimum	56.33	42.74	58.02	59.53
	Maximum	88.5	84.63	85.29	72.08
	Mean	79.19	67.09	77.03	67.85
	Standard Deviation	7.52	9.39	6.02	3.73

Along with intact rock properties, the joints and in situ stresses are the other parameters affecting the rock-mass behavior during the tunnel construction and the stress parameter is not taken into consideration in the RMR_{89} or RMR_{14} versions of the *RMR*. A different classification, known as SRC (surface rock classification), which has a relevant parameter for stresses based on tunnels experience in weak rocks [28], was used to capture the rock-mass behavior in the case of tunneling in a stressed environment. On considering the rating for stresses in SRC classification as a reference, a stress adjustment factor was suggested based on three hypotheses to extend the application of RMR_{89} systems in a highly stressed jointed rock-mass environment, as shown in Table 3 [16]. For this purpose, the difference between two values (calculated RMR_{89} through characterization and back-calculated *RMR* (*RMR**), i.e., (RMR_{89}–*RMR**)) was used for the extension of RMR_{89} in a high-stress environment using Equation (14), where $F_{stress-89}$ rating, depending on the strength–stress ratio and selection criterion, is shown in Table 4 [16].

$$RMR^{*}_{89} = RMR_{89} + F_{stress-89} \quad (14)$$

where RMR_{89}* is the stressed adjusted RMR_{89}.

Table 3. Hypothesis used for the stress adjustment factor for RMR_{89}.

Hypothesis		**Values of σ_c/σ_1**		
		5–4	**4–3**	**3–2**
1	$F_{stress-89}$	−5	−10	−15
2		−5	−10	−10
3		−10	−10	−10

Table 4. Stress adjustment factor selection for RMR_{89} and RMR_{14} based on the strength–stress ratio.

Range of Ratio σ_c/σ_1	**Rating**	
	***RMR*$_{89}$**	***RMR*$_{14}$**
5–4	−5	−22.326
4–3	−10	−27.169
3–2	−15	−32.012

The RMR_{14} system is in the development stage, and the support design chart is not revised thus far for this version of *RMR* [19]. However, as can be observed from the data in Table 2, the RMR_{14} values are higher than RMR_{89}, and a strong correlation exists between them [16,19]. The correlation between the two versions of *RMR* based on the data of the four projects is expressed in Equation (15). Taking into consideration this correlation equation, a stress adjustment factor is also suggested for RMR_{14}, as shown in Equation (16). The selection criterion for $F_{stress-14}$ in Equation (16) is shown in Table 4 based on the strength–stress ratio.

$$RMR_{14} = 0.9686 \times RMR_{89} + 17.483, \ (R^2 = 0.92) \tag{15}$$

$$RMR^*_{14} = RMR_{14} + F_{stress-14} \tag{16}$$

where RMR_{14}* is the stressed adjusted RMR_{14}.

Although a modified Q value (Q_c) is obtained owing to the additional normalized factor in Equation (13), the support chart remained unchanged. The resultant rock quality obtained from the back analysis can be defined as Q or Q_c. Equation (12) is rearranged to obtain Equation (17), and this equation was used for the *SRF* (SRF_Q) calculation for all the sections of the four projects while taking the back-calculated value as Q. If the back-calculated value is taken as Q_c, the normalized SRF_Q can then be calculated using Equation (18).

$$SRF_Q = \left(\frac{RQD}{J_n}\right) \times \left(\frac{J_r}{J_a}\right) \times \left(\frac{J_w}{Q}\right) \tag{17}$$

$$Normalized\ SRF_Q = SRF_Q \times \left(\frac{\sigma_c}{100}\right) \tag{18}$$

The known parameters for Equations (17) and (18) are shown in Table 5 for the four projects.

Table 5. Number of sections along with known parameters of tunneling quality index system for the four projects.

Project	No. of Sections	σ_c (MPa) (No. of Sections)								J_r	J_a	J_w
LT	258	75 (178)	65 (06)	60 (23)		56.25 (40)		37.5 (11)		3	1	1
NJHP	204	100 (44)	90 (20)	80 (31)	75 (04)	60 (07)	50 (66)	45 (11)	40(21)	1.5	3 2 1	1 0.66
KT	50	86 (15)				82 (35)				3	1	1 0.66
GGHP	30	75 (20)				54 (10)				3	1	1

During the back-calculation of the rock-mass quality (*RMR** and *Q**), there is no criterion for the rock-bolt-based back-calculated rock-mass quality (RMR_1* and Q_1*) and shotcrete along with tunnel-span-back-calculated rock-mass quality (RMR_2* and Q_2*) weightage. Owing to this limitation, five different cases, as described in Table 6, are adopted to indicate the weightage effect on the RMR_{89} and *RMR** difference (RMR_{89}-*RMR**), and RMR_{89} and RMR_{89}* difference (RMR_{89}-RMR_{89}*). Similarly, for each case of Table 6, the weightage effect on the RMR_{14} and *RMR** difference (RMR_{14}-*RMR**), and RMR_{14} and RMR_{14}* difference (RMR_{14}-RMR_{14}*) is also determined. For Q system, each case of weightage in Table 6 was selected, and the back-calculated Q* value was used in Equation (17) for the SRF_Q calculation. The weightage effect is determined during the plotting SRF_Q versus the relative block sizes (RQD/J_n) for the different ranges of the strength–stress ratio. The procedure for the calculation of *RMR** and Q* for five different weightage cases of Table 6 are illustrated in Example 1, and the obtained results are summarized in Table 7. For this illustration, a 10 m span tunnel with

two different support scenarios in terms of rock bolt spacing and fiber-reinforced shotcrete thickness are used.

Table 6. Five different cases for calculating *RMR** and *Q** (Figure 1) while considering the weightage of the rock-mass quality obtained from rock bolts spacing and shotcrete thickness along with tunnel span.

Case No.	Weightage of RMR_1* and Q_1*	Weightage of RMR_2* and Q_2*
1	100	Actual *
2	75	50
3	50	50
4	50	75
5	50	100

* Explained in Example 1.

Table 7. Back-calculated rock-mass quality values for two different scenarios of Example 1 based on the weightage cases of Table 6.

Case No.	Scenario 1		Scenario 2	
	*RMR**	*Q**	*RMR**	*Q**
1	55.55	2.77	47.55	0.60
2	54.16	2.52	48.0	0.64
3	52.30	2.15	48.50	0.70
4	50.44	1.78	49.0	0.76
5	49.2	1.53	49.33	0.80

Example 1.

Installed support scenario 1

Shotcrete thickness = 12 cm
Rock bolt spacing = 2.1 m
RMR_1 and Q_1* = 61.6 and 4, respectively.*
RMR_2 and Q_2* = 43 and 0.3 respectively*
Percentage of RMR contribution in shotcrete thickness = 48.254
Percentage of Q contribution in shotcrete thickness = 50

Installed support scenario 2

Shotcrete thickness = 9 cm
Rock bolt spacing = 1.5 m
RMR_1 and Q_1* = 46 and 0.4, respectively.*
RMR_2 and Q_2* = 51 and 1.0 respectively*
Percentage of RMR contribution in shotcrete thickness = 44.745
Percentage of Q contribution in shotcrete thickness = 50

3. Results

The rock-mass quality was calculated using Equation (1) for the 542 tunnel sections of the four tunnel projects following the two approaches of calculating rock-mass quality through characterization (RMR_{89}) and back-calculation (*RMR**). All the five cases of Table 6 were considered in the *RMR** calculation. Of the 542 tunnel sections, 468 sections show that RMR_{89} > *RMR** for all the five cases

of weightage. The cases that show the difference (RMR_{89}-RMR*) as a positive value are plotted in Figure 2.

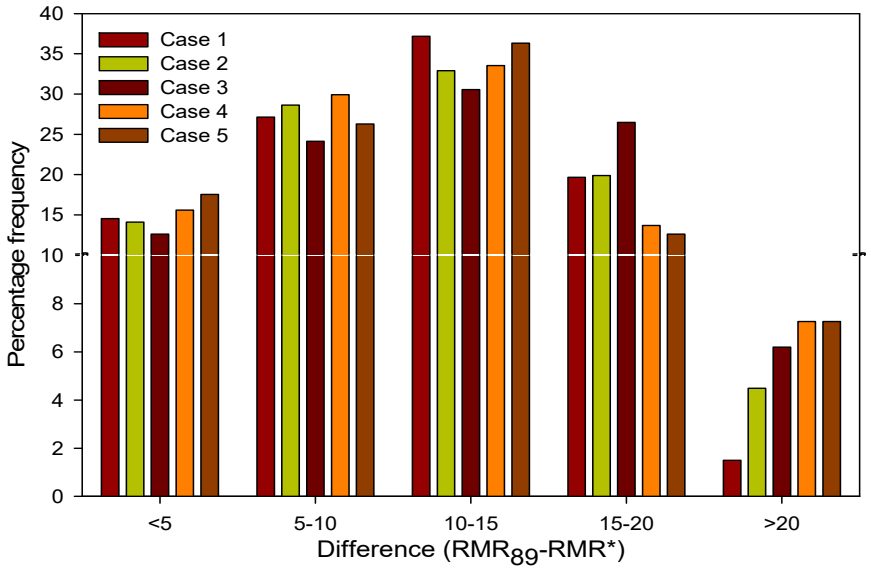

Figure 2. Percentage frequency of the calculated RMR_{89} and back-calculated RMR difference considering the five cases of Table 6.

To evaluate the effect of the weightage for all the five cases in the stress adjustment factor for RMR_{89}, three hypotheses were adopted for the $F_{stress-89}$. These hypothesis were also used for the extension of the RMR_{89} application for the rock-mass quality determination in highly stressed jointed rock-mass environments [16]. The details of the hypothesis tested for the rating selection based on intact rock strength to major principal stress (σ_1) ratio (σ_c/σ_1) are shown in Table 3.

Using Equation (14), after applying the stress adjustment factor $F_{stress-89}$, based on the selection criterion expressed in Table 3 for all the 468 tunnel sections, RMR_{89} was adjusted for the stress parameter (RMR_{89}*). The RMR* was calculated using five different weightages of Table 6. For each case, the RMR_{89}* and RMR* are compared in terms of their difference (RMR_{89}*-RMR*) for all the five cases of weightage and for three hypotheses and the obtained results are expressed in Figure 3.

In case of RMR_{14}, the rock-mass quality was calculated using Equation (5) for the 542 tunnel sections of the four tunnel projects through characterization and was compared with the back-calculated RMR while considering all the five cases of Table 6. The comparison between the calculated RMR (RMR_{14}) and back-calculated RMR (RMR*) for all the sections reveal that $RMR_{14} > RMR$* for all the five cases, and the details in terms of their difference (RMR_{14}-RMR*) are shown in Figure 4.

To evaluate the effect of the weightage for all the five cases in the stress adjustment factor for RMR_{14}, the three hypotheses were considered for the stress adjustment factor ($F_{stress-14}$). The details of the hypothesis tested for the rating selection based on (σ_c/σ_1) for RMR_{14} are summarized in Table 8.

Using Equation (16), after applying the stress adjustment factor based on the selection criterion expressed in Table 7 for all the tunnel sections, RMR_{14} was adjusted for a stress parameter as RMR_{14}* using Equation (16). The stress-adjusted RMR_{14} (RMR_{14}*) and RMR* are compared in terms of their difference (RMR_{14}*-RMR*) for all the five cases of weightage and for the three hypotheses, and the obtained results are expressed in Figure 5.

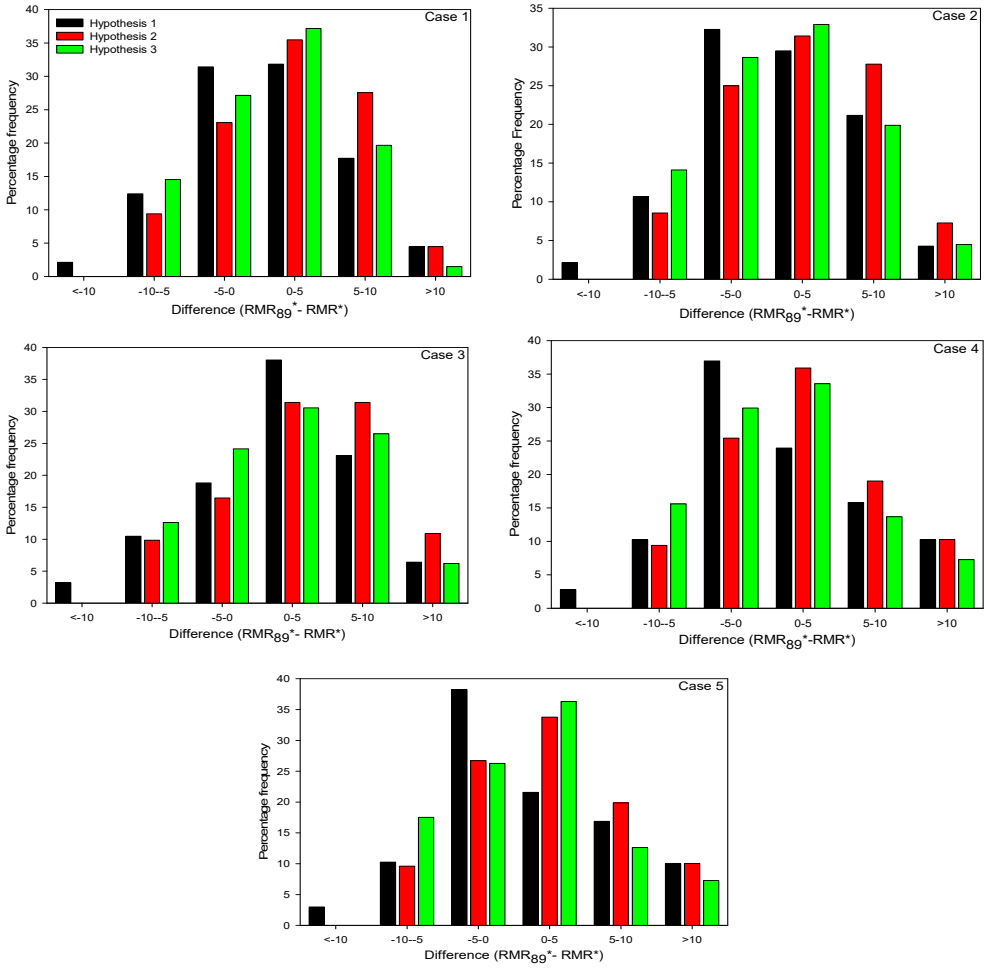

Figure 3. Effect of weightage (Table 6) during back-calculation of rock-mass quality (*RMR**) (Figure 1) in terms of difference between stress-adjusted RMR_{89} (RMR_{89}*) and *RMR** using hypothesis of Table 3.

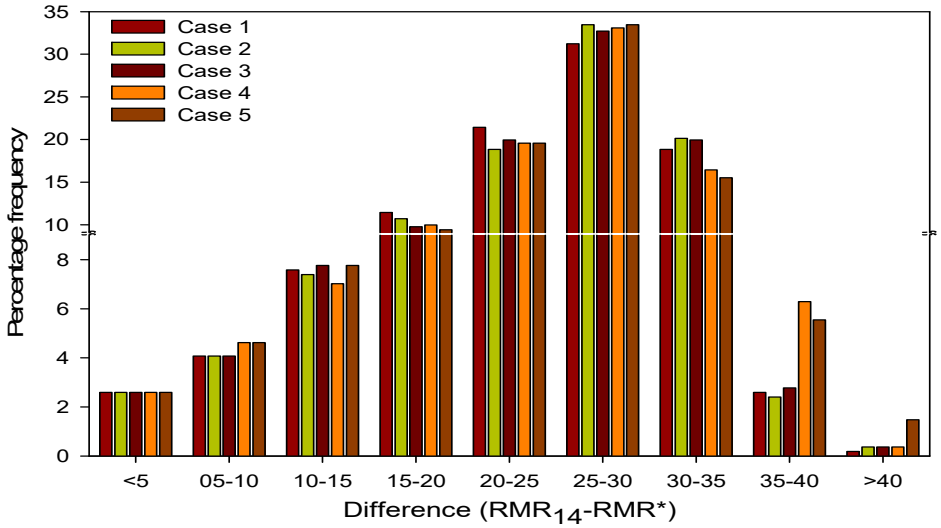

Figure 4. Percentage frequency of the calculated RMR_{14} and back-calculated *RMR* (*RMR**) difference considering the five cases of Table 6.

Table 8. Hypothesis used for the $F_{stress-14}$ in tunnel support design.

Hypothesis		Values of σ_c/σ_1		
		4–5	**3–4**	**2–3**
1	$F_{stress-14}$	−22.326	−27.169	−32.012
2		−22.326	−27.169	−27.169
3		−27.169	−27.169	−27.169

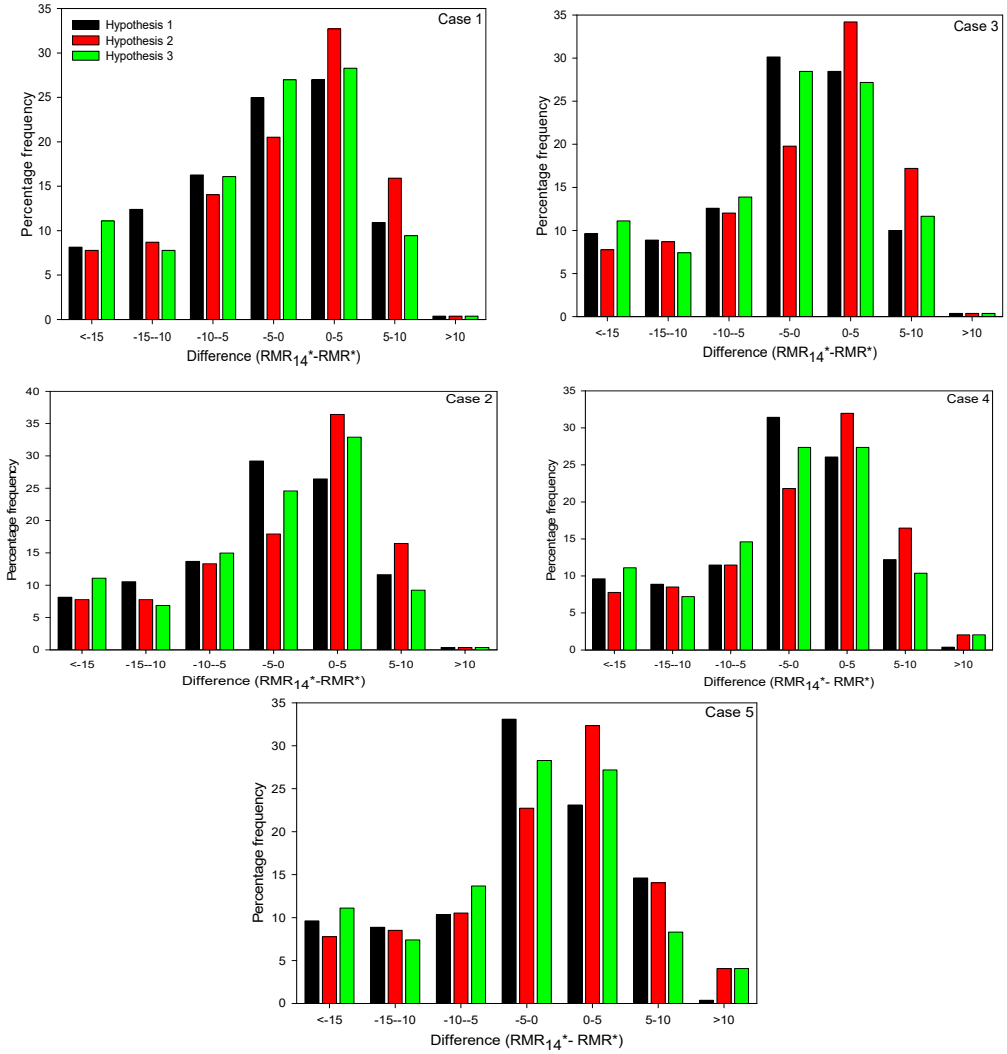

Figure 5. Effect of weightage (Table 6) during back-calculation of rock-mass quality (*RMR**) (Figure 1) in terms of difference between stress-adjusted RMR_{14} (RMR_{14}*) and *RMR** using hypothesis of Table 7.

The data of the 542 tunnel sections (as summarized in Table 5) were used in Equation (17). For Equation (17), the back-calculation rock-mass quality (Q*) was determined using the five different weightages of Q_1* and Q_2* as per the details in Table 6. On separating the number of cases based on σ_c/σ_1 from the 542 sections, 156 tunnel sections were found to have this ratio in the range of 4 to 5. In the range of 3 to 4, 232 cases exist, and the remaining 154 sections have a strength–stress ratio in the range of 2 to 3. Cases 1 and 3 of Table 6 are already respectively used for the extension of the application of the Q system of Barton and the rock-mass index (*RMi*) system of Palmstorm for a highly stress-jointed rock-mass environment [16,17]. The back-calculated rock-mass quality in Figure 1 for all the five cases of weightage was taken as the Q value in Equation (17) for the calculation of the *SRF* (SRF_Q). This SRF_Q was plotted against the relative block size (RQD/J_n) for different ranges of

strength–stress ratio for all the five cases of Q^* based on their weightage (Table 6). The results are shown in Figure 6. The best fit equation for Case 1 is Equation (19), and for the remaining four cases is Equation (20). Equations (19) and (20) are already suggested for Case 1 and 3, respectively [16,17]. For Case 2, the best fit Equation (20) has the same values for the constant α. However, in Cases 4 and 5, the constant α values are different, as shown in Figure 6.

$$SRF_Q = 2.054 \exp\left(0.205 \frac{RQD}{J_n}\right) + 14.865 \exp\left(-0.41 \frac{\sigma_c}{\sigma_1}\right) \quad (19)$$

$$SRF_Q = 2.0 \times \exp\left(0.21 \times \frac{RQD}{J_n}\right) + 12.0 \times \exp\left(-\alpha \times \frac{\sigma_c}{\sigma_1}\right) \quad (20)$$

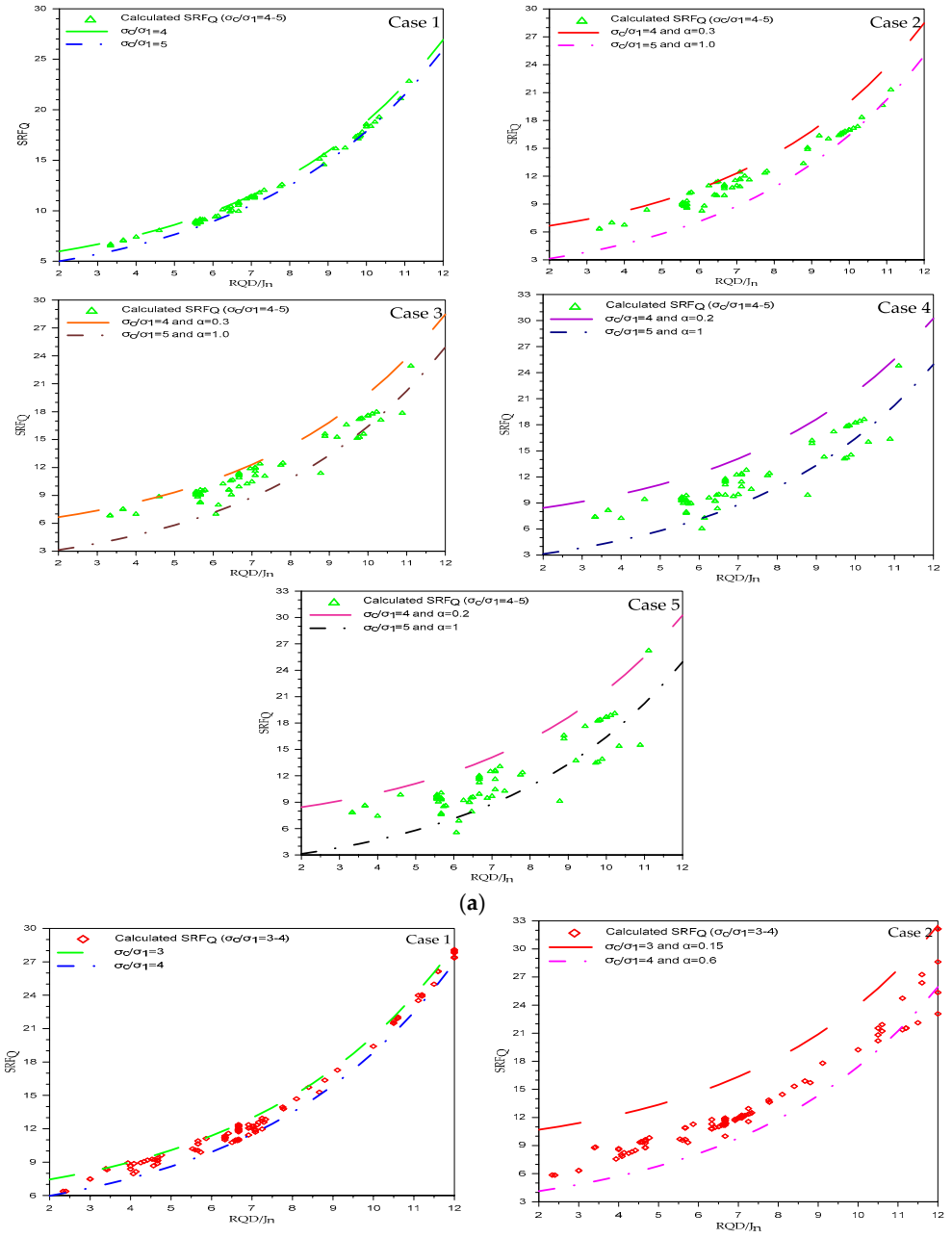

(**a**)

Figure 6. *Cont.*

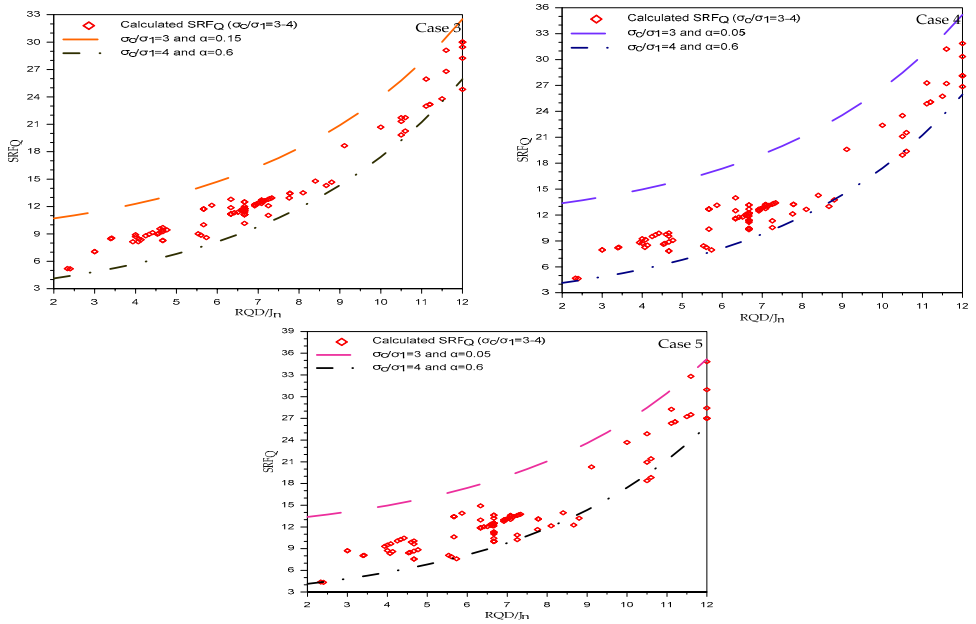

(**b**)

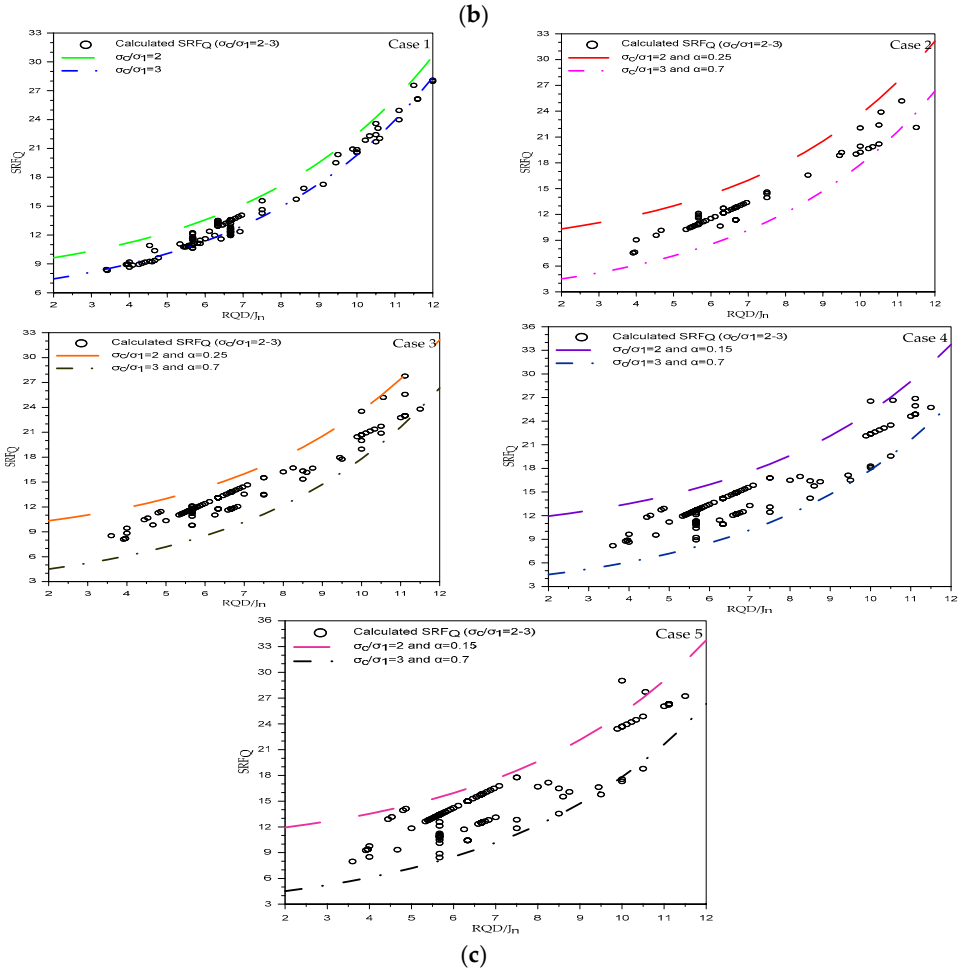

(**c**)

Figure 6. Effect of weightage (Table 6) during back-calculation of rock-mass quality index value (Q*) (Figure 1) in SRF_Q versus RQD/Jn plots for different ranges of strength–stress ratio. (**a**) σ_c/σ_1 = 4–5, (**b**) σ_c/σ_1 = 3–4, (**c**) σ_c/σ_1 = 2–3.

4. Discussion

The already supported tunnel sections data is used in this article. The same data is used for the extension of the RMR [18,19], tunneling quality index [12,26], and RMR index [29] in highly stressed jointed rock-mass environments [16,17]. For the extension process, the back-calculation approach is used for the calculation of the rock-mass quality. In the back-calculation approach, the rock bolt spacing and shotcrete thickness are used along with the tunnel span for determining the rock-mass quality. As can be observed from Figure 1, the final rock-mass quality depends on the rock-mass quality obtained from the rock bolt spacing and shotcrete thickness in combination with the tunnel size. Although the average weightage is used for the calculation of the final rock-mass quality, owing to the unavailability of any criterion, the different weightage effect was not studied. Therefore, five different weightages were selected for the final rock-mass quality determination as shown in Table 6, and the obtained results are presented. For illustration, an example is used, the results of which are summarized in Table 7.

Approximately 86% of the data shows that the back-calculated *RMR* (*RMR**) is lower than the calculate *RMR* (RMR_{89}) obtained using Equation (1), which indicates that the RMR_{89} suggested supports are lighter than the actual support. This difference is shown in Figure 2 in terms of the difference between RMR_{89} and *RMR** and reveals that for all cases of weightage, this difference is highest in the rage of 10 to 15 points of *RMR*. In each range of difference (<5, 5–10, 10–15, 15–20, and >20) the average vales for the five cases are 14.87, 27.22, 34.10, 18.46, and 5.34 with a standard deviation of 1.83, 2.21, 2.68, 5.59, and 2.43, respectively. This shows that for all the five ranges of differences, the deviation from the average of the five cases is very low except in the case of the range of 15–20, wherein the deviation is 5.59. This high deviation is due to the higher frequency of Case 3 with respect to other cases in the range 15–20. The percentage frequency of the difference between RMR_{89} and *RMR** (RMR_{89}-*RMR**) in the range of 5 to 20 decreases with the case number, and these values are 84, 82, 81, 77, and 75 for Case 1—5, respectively. As the weightage of the rock-bolts-based back-calculated *RMR* (RMR_1*) decreased along with the increase in the shotcrete-based *RMR* (RMR_2*), the percentage frequency decreased. This decrease is due to the higher value of RMR_1* than RMR_2* in the maximum tunnel sections. After the application of the stress adjustment factor based on the strength–stress ratio as per the guidelines of Table 3, the percentage frequency of the difference between the stress-adjusted *RMR* (RMR_{89}*) and *RMR** is the greatest in the range of −5 to 5 for all the five cases of the weightage except Case 3 and Hypothesis 2, as shown in Figure 3. For this case, the percentage frequency is 48 for (RMR_{89}*-*RMR**) in the range of −5 to 5. Hypothesis 1 of Table 3 was selected as the stress adjustment factor based on strength–stress ratio obtained for RMR_{89} [16]. The leading case in terms of percentage frequency, where (RMR_{89}*-*RMR**) is in the range of −5 to 5 for Hypothesis 1, is Case 1 followed by Cases 2–5. Their values are 63, 62, 61, 60, and 57, respectively.

RMR_{14} is the latest version of the *RMR* system, and therefore, the result of this version and *RMR** are compared for each section and expressed in Figure 4 in terms of their difference. In each range of difference, in Figure 4, the percentage frequency of each case is very close with a very low value of standard deviation. The maximum standard deviation is obtained for the difference range 30–35 with a value of 2.09 from the average value of 18.19. As the RMR_{14} values are higher than RMR_{89}, as shown in Table 2 and Equation (15), the difference (RMR_{14}-*RMR**) is greater than that between RMR_{89} and *RMR** (RMR_{89}-*RMR**), as shown in Figure 4. Figure 4 reveals that for all the cases of weightage, this difference (RMR_{14}-*RMR**) is greatest in the range of 20 to 35 points of *RMR*. In terms of the percentage frequency, their values are 72, 72, 73, 69, and 69 for Cases 1–5, respectively. Based on the correlation Equation (15), RMR_{14} decreases significantly with the stress adjustment factor for all the hypotheses of Table 8. After the application of the stress adjustment factor based on the strength–stress ratio as per the guidelines of Table 8, the percentage frequency of the difference between the stress-adjusted RMR_{14} (RMR_{14}*) and *RMR** is greatest in the range of −5 to 5 following all the five cases of weightage. Hypothesis 1 of Table 7 for Case 3 is used for the stress adjustment factor for RMR_{14} [16]. The leading case in terms of the percentage frequency for the difference between

RMR_{14}* and RMR_{14} (RMR_{14}*-*RMR**) in range of −5 to 5 is Case 3 with a value of 58.6 followed by Cases 1, 2, 4, and 5 with values of 57.5, 56.2, 55.6, and 51.9, respectively. Comparing this difference (RMR_{14}*-*RMR**) with the difference in RMR_{89} (RMR_{89}*-*RMR**), the percentage frequency in the range of −5 to 5 is lower. These lower values are due to the selection of the stress adjustment factor based on the correlation equation, wherein the data are somewhat scattered from the trend line ($R^2 < 1.0$). Secondly, on comparing Figures 3 and 5, the difference in the RMR_{14} case is more on the negative side as compared to the difference in RMR_{89}, wherein the difference is more on the positive side.

According to the Grimstad and Barton [30], massive rocks have a greater probability of the occurrence of rock burst in a high-stress environment and suggest a higher rating for the *SRF* in their revised criterion based on relative block size. Their criterion is used for the rock burst occurrence evaluation [31]. In case of a jointed rock mass under high stresses, the *SRF* is the function of the strength–stress ratio and relative block size along with the intact rock strength [16,17]. The effect of the weightage during the determination of the rock-mass quality through back-calculation as per the details of Table 6 along with procedure of Figure 1 and their corresponding effect on the *SRF* value using Equation (17) are shown in Figure 6. The line trends in all five cases show that the rate of increase in *SRF* with the relative block size increases. In Case 1, the variation of *SRF* is 20.95 for RQD/Jn from 2 to 12 for all the three ranges of the strength–stress ratio. The Case 1, Figure 6a–c shows that as the strength–stress ratio range changes from 2–3 to 3–4 and then 4–5, the difference between the trend lines for any given value of relative size decreases. These values are 2.2, 1.46, and 0.97, respectively. In all the remaining cases, the differences are controlled by the difference in values of the constant α in each case and the strength–stress ratio range. In each range of the strength–stress ratio, Cases 2 and 3 have the same difference in α. Similarly, Cases 4 and 5 have the same difference in α. For Cases 2 and 3, the differences in α are 0.7, 0.45, and 0.45 for the strength–stress ratios 4–5, 3–4, and 2–3, respectively. For Cases 4 and 5, these differences are 0.8, 0.55, and 0.55, respectively. The difference in the trend line in Figure 6a shows that for any values of relative block sizes, the difference between the *SRF* for strength–stress ratios 3 and 2 are 5.81 for Cases 2 and 3 and 7.42 for Cases 4 and 5. In Figure 6b, where the trend lines are shown for strength–stress ratios of 3 and 4, the difference between the *SRF* increases for the given value of the relative block size. These values are 6.56 for Cases 2 and 3 and 9.24 for Cases 4 and 5. In Figure 6c, where the trend lines are shown for the strength–stress ratios of 4 and 5, the difference between the *SRF* decreases for the given value of the relative block size. The difference between the *SRF* for any given value of *RQD/Jn* are 3.53 for Cases 2 and 3 and 5.3 for Cases 4 and 5.

5. Conclusions

The following conclusions are obtained from this study:

1. During the back-calculation of the rock-mass quality (*RMR** and *Q**), the difference between the rock-mass quality obtained from the rock bolt spacing (RMR_1* and Q_1*) and fiber-reinforced shotcrete thickness along with the tunnel span (RMR_2* and Q_2*) are responsible for the weightage effect. The weightage effect is more pronounced when the difference between the back-calculated rock-mass quality from the rock bolts spacing and shotcrete thickness is high and vice versa.
2. So far, the back-calculation approach is used for the extension of empirical classification systems to highly stress-jointed rock-mass environment and due to low difference between the back-calculated rock-mass quality through different support media, the weightage effect is small. However, using this approach for the extension of *RMR* and *Q* systems to other ground behaviors during tunnel construction and stability, selection of appropriate weightage is the key to evaluate the contribution of rock bolt and shotcrete.
3. By increasing the weightage of the shotcrete along with the tunnel-span-based back-calculated rock-mass quality (RMR_2* and Q_2*), the *RMR** and *Q** values are high if RMR_2* > RMR_1* and Q_2* > Q_1* and vice versa. Owing to the structure of *RMR* and *Q* value calculation in the two systems, the consequence of low weightage effect is higher in the *Q* system as compared to the *RMR* system.

4. In the case of the Q system, on using the five weightage cases, the plot trend of the stress reduction factor SRF_Q versus the relative block size RQD/J_n is the same for all the three ranges of strength–stress ratio (σ_c/σ_1). These trends show that the rate of SRF_Q increases with the relative block size.

Author Contributions: H.Y. supervised the research. J.K. and H.R. have developed the proposed research concept. W.A. contributed to reviewing the final paper and made important suggestions and recommendations for paper revision. A.M.N. helped in writing and re-checking the paper technically as well as grammatically.

Funding: This research was funded by Ministry of Land, Infrastructure and Transport of the Korean government grant number 19SCIP-B089413-06.

Acknowledgments: This research was supported by the "Development of Design and Construction Technology for Double Deck Tunnel in Great Depth Underground Space (19SCIP-B089413-06)" from Construction Technology Research Program funded by Ministry of Land, Infrastructure and Transport of the Korean government. The authors (Hafeezur Rehman, Wahid Ali and Abdul Muntaqim Naji) are extremely thankful to the Higher Education Commission (HEC) of Pakistan for HRDI-UESTPs scholarship.

Conflicts of Interest: The authors declare no conflict of interest.

References

1. Zheng, Z.; Xu, Y.; Li, D.; Dong, J. Numerical analysis and experimental study of hard roofs in fully mechanized mining faces under sleeve fracturing. *Minerals* **2015**, *5*, 758–777. [CrossRef]
2. Li, Y.; Jin, X.; Lv, Z.; Dong, J.; Guo, J. Deformation and mechanical characteristics of tunnel lining in tunnel intersection between subway station tunnel and construction tunnel. *Tunn. Undergr. Space Technol.* **2016**, *56*, 22–33. [CrossRef]
3. Naji, A.M.; Emad, M.Z.; Rehman, H.; Yoo, H. Geological and geomechanical heterogeneity in deep hydropower tunnels: A rock burst failure case study. *Tunn. Undergr. Space Technol.* **2019**, *84*, 507–521. [CrossRef]
4. Rehman, H.; Ali, W.; Naji, A.; Kim, J.-J.; Abdullah, R.; Yoo, H.-k. Review of rock-mass rating and tunneling quality index systems for tunnel design: Development, refinement, application and limitation. *Appl. Sci.* **2018**, *8*, 1250. [CrossRef]
5. Huo, J.; Zhu, D.; Hou, N.; Sun, W.; Dong, J. Application of a small-timescale fatigue, crack-growth model to the plane stress/strain transition in predicting the lifetime of a tunnel-boring-machine cutter head. *Eng. Fail. Anal.* **2017**, *71*, 11–30. [CrossRef]
6. Huo, J.; Wang, W.; Sun, W.; Ling, J.; Dong, J. The multi-stage rock fragmentation load prediction model of tunnel boring machine cutter group based on based on dense core theory. *Int. J. Adv. Manuf. Technol.* **2017**, *90*, 277–289. [CrossRef]
7. Mazaira, A.; Konicek, P. Intense rockburst impacts in deep underground construction and their prevention. *Can. Geotech. J.* **2015**, *52*, 1426–1439. [CrossRef]
8. Palmstrom, A.; Stille, H. Ground behaviour and rock engineering tools for underground excavations. *Tunn. Undergr. Space Technol.* **2007**, *22*, 363–376. [CrossRef]
9. Stille, H.; Palmström, A. Ground behaviour and rock mass composition in underground excavations. *Tunn. Undergr. Space Technol.* **2008**, *23*, 46–64. [CrossRef]
10. Santos, V.; da Silva, P.F.; Brito, M.G. Estimating rmr values for underground excavations in a rock mass. *Minerals* **2018**, *8*, 78. [CrossRef]
11. Bieniawski, Z. Engineering classification of jointed rock masses. *Civ. Eng. South Afr.* **1973**, *15*, 333–343.
12. Barton, N.; Lien, R.; Lunde, J. Engineering classification of rock masses for the design of tunnel support. *Rock Mech.* **1974**, *6*, 189–236. [CrossRef]
13. Rehman, H.; Naji, A.; Kim, J.-J.; Yoo, H.-K. Empirical evaluation of rock mass rating and tunneling quality index system for tunnel support design. *Appl. Sci.* **2018**, *8*, 782. [CrossRef]
14. Palmstrom, A.; Broch, E. Use and misuse of rock mass classification systems with particular reference to the q-system. *Tunn. Undergr. Space Technol.* **2006**, *21*, 575–593. [CrossRef]
15. Oreste, P. Analysis of structural interaction in tunnels using the covergence–confinement approach. *Tunn. Undergr. Space Technol.* **2003**, *18*, 347–363. [CrossRef]

16. Rehman, H.; Naji, A.M.; Kim, J.-J.; Yoo, H. Extension of tunneling quality index and rock mass rating systems for tunnel support design through back calculations in highly stressed jointed rock mass: An empirical approach based on based on tunneling data from himalaya. *Tunn. Undergr. Space Technol.* **2019**, *85*, 29–42. [CrossRef]
17. Lee, J.; Rehman, H.; Naji, A.; Kim, J.-J.; Yoo, H.-K. An empirical approach for tunnel support design through q and rmi systems in fractured rock mass. *Appl. Sci.* **2018**, *8*, 2659. [CrossRef]
18. Bieniawski, Z.T. *Engineering Rock Mass Classifications: A Complete Manual for Engineers and Geologists in Mining, Civil, and Petroleum Engineering*; John Wiley & Sons: Hoboken, NJ, USA, 1989.
19. Celada, B.; Tardáguila, I.; Varona, P.; Rodríguez, A.; Bieniawski, Z. Innovating Tunnel Design by an Improved Experience-Based RMR System. In Proceedings of the World Tunnel Congress, Foz do Iguaçu, Brazil, 9–15 May 2014; p. 9.
20. Bieniawski, Z. Geomechanics classification of rock masses and application in tunneling. In Proceedings of the 3rd International Congress on Rock Mechanics, Denver, CO, USA, 1–7 September 1974; pp. 27–32.
21. Bieniawski, Z. Case studies: Prediction of rock mass behaviour by the geomechanics classification. In Proceedings of the Second Australia-New Zealand Conference on Geomechanics, Brisbane, Australia, 21–25 July 1975; Institution of Engineers, Australia: Brisbane, Australia, 1975; p. 36.
22. Bieniawski, Z. The geomechanics classification in rock engineering applications. In Proceedings of the 4th ISRM Congress, Montreux, Switzerland, 2–8 September 1979; International Society for Rock Mechanics: Salzburg, Austria, 1979.
23. Bieniawski, Z. Misconceptions in the applications of rock mass classifications and their corrections. In Proceedings of the ADIF Seminar on Advanced Geotechnical Characterization for Tunnel Design, Madrid, Spain, 29 June 2011; pp. 4–9.
24. Lowson, A.; Bieniawski, Z. Critical assessment of rmr based-based tunnel design practices: A practical engineer's approach. In Proceedings of the SME, Rapid Excavation and Tunnelling Conference, Washington, DC, USA, 23–26 June 2013; pp. 180–198.
25. Bieniawski, Z.T.; Aguado, D.; Celada, B.; Rodriquez, A. Forecasting tunnelling behaviour. *T T Int.* **2011**, 39–42.
26. Barton, N. Some new q-value correlations to assist in site characterisation and tunnel design. *Int. J. Rock Mech. Min. Sci.* **2002**, *39*, 185–216. [CrossRef]
27. NGI. The q-System, Rock Mass Classification and Support Design. Available online: https://www.ngi.no/eng/Publications-and-library/Books/Q-system (accessed on 9 April 2018).
28. De Vallejo, L.G. Src rock mass classification of tunnels under high tectonic stress excavated in weak rocks. *Eng. Geol.* **2003**, *69*, 273–285. [CrossRef]
29. Palmstrom, A. *Rmi—A Rock Mass Characterization System for Rock Engineering Purposes*; Oslo University: Oslo, Norway, 1995.
30. Grimstad, E.; Barton, N. Updating the q-system for nmt. In Proceedings of the International Symposium on Sprayed Concrete-Modern Use of Wet Mix Sprayed Concrete for Underground Support, Fagemes, Oslo, Norway, 20–24 June 1993; Norwegian Concrete Association: Fagemes, Oslo, Norway, 1993.
31. Naji, A.; Rehman, H.; Emad, M.; Yoo, H. Impact of shear zone on rockburst in the deep neelum-jehlum hydropower tunnel: A numerical modeling approach. *Energies* **2018**, *11*, 1935. [CrossRef]

© 2019 by the authors. Licensee MDPI, Basel, Switzerland. This article is an open access article distributed under the terms and conditions of the Creative Commons Attribution (CC BY) license (http://creativecommons.org/licenses/by/4.0/).